APPLICATION OF FDS AND FIREFOAM IN LARGE EDDY SIMULATIONS OF A TURBULENT BUOYANT HELIUM PLUME

G. Maragkos*, P. Rauwoens* and B. Merci*
Georgios.Maragkos@UGent.be
* Department of Flow, Heat and Combustion Mechanics, Ghent University, St. Pietersnieuwstraat 41, B-9000, Ghent, Belgium

Abstract
Large eddy simulations are conducted in the near-field region of a large turbulent buoyant helium plume. Such plumes are of relevance for fire safety research due to the similar flow features as in the buoyant (smoke) plumes above the fire source. The transient and mean flow dynamics are discussed with and without the use of Smagorinsky type sub-grid scale (SGS) model. For this purpose two different CFD packages are used. Small-scale structures, formed at the edge of the plume inlet due to a baroclinic and gravitational mechanism and subject to flow instabilities, interact with large-scale features of the flow, resulting in a puffing cycle. This puffing cycle is recovered in the simulations. In general, the LES calculations reproduce the main features of the turbulent plume. Mean velocity results compare well with the experimental data. The mass fractions are over-predicted on the centreline though, higher on the domain.

Introduction
Buoyant plumes are encountered in a diverse range of engineering and environmental processes, including pool fires, atmospheric exhaust phenomena like smokestacks and gas releases in geothermal events. Therefore it is of great interest to develop a better understanding of the unstable behavior and flow evolution of such plumes. The specific motivation for this study is to perform numerical simulations of a flow with turbulent mixing characteristics that are similar to large-scale fires. For this reason, large eddy simulations (LES) are performed in the near field region of a large axisymmetric turbulent buoyant helium plume with two different computational fluid dynamics (CFD) packages that are often used in the fire science community: FireFOAM [1] and FDS 5 [2]. The use of Smagorinsky type sub-grid scale (SGS) models is also analyzed with respect to their influence on the flow dynamics.

The study of turbulent buoyant plumes is particularly difficult for several reasons. A rapid transition of the flow, from laminar to fully turbulent, is encountered in the plume, usually within a few inlet diameters from the source. Once turbulent, plumes are characterized by large-scale vorticity created as a result of buoyancy and shear forces arising from the interaction of the jet with the ambient fluid. Two modes of turbulence are important [3] in this kind of flows. First, the classical Rayleigh - Taylor instability causes helium bubbles and air spikes at the plume base and the large scale puffing often seen in buoyant plumes. Baroclinic and gravitational torques, arise near the edge of the inlet from a misalignment of pressure and gravity respectively, with density gradients, which produce a Rayleigh - Taylor instability at the base of the plume. Velocity and density fluctuations first appear at the smallest scales, rapidly grow in size and magnitude and eventually interact with the large-scale motion of the turbulent flow, leading to the vortex that grows to dominate the flow. In addition, Kelvin-Helmholtz instabilities arise at the two fluid interfaces from velocity shear. An inverse energy cascade of kinetic and scalar energies is created by these instabilities, which energize large-

scale structures as the plume rises from its base. The interaction of buoyancy forces with vorticity generates a characteristic "puffing" motion, by which entrained fluid periodically forces a mass of lighter fluid accumulating near the plume base upward through the overlying heavier fluid creating a toroidal vortex [4, 5]. In cases where the Reynolds and Richardson numbers are large enough, these unstable modes may be altered by intermittent secondary toroidal vortices that make the puffing irregular, and which amplify the entrainment rates and thus strongly alter the plume dynamics overall. The puffing cycles encountered in turbulent buoyant plumes are just one example of the very complex interaction between small and large-scale features of the turbulent flow.

In this kind of flows the coupling mechanism through density between the scalar field (species) and the momentum field is important since the mixture composition determines density through the mixture molecular weight. For buoyant, low Mach-number flows, the source term in the momentum equations is the product of density multiplied by gravity, hence, the forcing function for a buoyant flow. This buoyant forcing results in mixing that in turn changes density and thus the two sets of equations are coupled. Turbulence resulting directly from this coupling is referred to as "buoyancy generated turbulence" [6]. It is postulated in [7] that the turbulence arises due to a combination of strong buoyant vorticity generation and vorticity transport mechanisms that lead to entanglement of the vorticity resulting in a turbulent field. In RANS (Reynolds-Averaged Navier-Stokes) simulations the turbulence model needs to be adjusted to take this effect into account [8]. In LES, in principle this should be captured automatically. Yet, as explained later, this is not straightforward either.

In this study, large eddy simulations (LES) performed with FireFOAM and the fire dynamics simulator (FDS 5) will be compared with the well-documented experiment performed by O`Hern et al. [9]. FireFOAM is based on the OpenFOAM [10] platform, which is a set of object-oriented open source CFD toolboxes written in C++. It utilizes the finite volume method on unstructured polyhedral meshes and is highly scalable on massively parallel computers. An objective of this study is also to validate FireFOAM for buoyancy driven flows. By validating the code in a non-reacting plume, the effect of buoyancy-generated turbulence can be tested independent of the complexity introduced by turbulent combustion. Chung & Devaud et al. [11] studied the near field of the helium plume with traditional eddy-viscosity LES methods using FDS.

The SGS turbulence models are implemented differently in FDS and FireFOAM. In order to eliminate these differences, the comparison is made switching off the turbulence model. In FDS, this corresponds to the use of a Smagorinsky constant $c_s = 0$. For FDS, results are also shown with SGS model, with $c_s = 0.1$, for comparison purposes.

FireFOAM

In this study, a modified version of FireFOAM is used. The original mixture fraction equation is replaced by a "fuel" mass fraction equation and mixture density is calculated as a linear function of "fuel" and air mass fractions. Also the energy equation is not solved. FireFOAM solves for the low-Mach number form of the Navier-Stokes equations, using Favre-filtered quantities [12], along with a transport equation for "fuel" mass fraction and pressure for a non reacting, isothermal system with equal diffusivities and unity Lewis number.

Filtered density, $\bar{\rho}$, is a function of fuel and air composition. Thus the mixing induced by the momentum equations yields:

$$\bar{\rho} = \bar{\rho}_f \phi_f + \bar{\rho}_{air}(1 - \phi_f) \tag{6}$$

where ϕ_f is the volume fraction of helium and $\bar{\rho}_f$, $\bar{\rho}_{air}$ are the filtered densities of fuel and air respectively, calculated by the ideal gas law. The mass fraction of fuel, solved by the transport equation, is related to its volume fraction as:

$$Y = \frac{\bar{\rho}_f \phi_f}{\bar{\rho}_f \phi_f + \bar{\rho}_{air}(1-\phi_f)} \tag{7}$$

Densities of air and fuel are $\bar{\rho}_{air} = 0.987\,kg/m^3$ and $\bar{\rho}_f = 0.186\,kg/m^3$, calculated by the experimental conditions presented in the following section. Laminar viscosity is calculated by the experimental inlet Reynolds number, taken the value $\mu = 1.877 \times 10^{-5}\,kg/ms$, while the molecular Schmidt number is $Sc = 0.2$ [13].

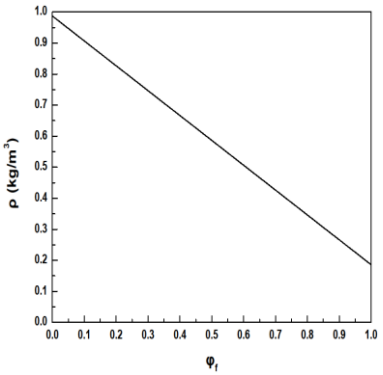

Figure 1. Density as a function of fuel volume fraction ϕ_f

Total pressure $\bar{p}$ is expressed as:

$$\bar{p} = \bar{p}_o + \bar{\rho} g_i x_i \tag{8}$$

with $\bar{p}_o$ the reference pressure, g_i the gravity vector and x_i the distance from the plume inlet. Due to the low Mach number approximation considered in the study, dynamic pressure $\bar{p}_d$ is not taken into account in the calculation of the total pressure $\bar{p}$, but only used in the predictor and corrector step of the momentum equations.

Fire Dynamics Simulator (FDS)

FDS solves for the low-Mach number form of the Navier-Stokes equations along with an equation for chemical species and energy. The ideal gas law couples temperature, density and pressure, with the chemical species mass fraction being incorporated in the pressure term. For a better description of the equations and the approximations used in the FDS code the reader can refer to Anderson et al. [14]. The filtering process in LES introduces unclosed quantities that are not resolved, such as the SGS stress terms, the SGS heat and mass flux, the combustion heat release rate and the radiation loss that have to be modeled. The system considered here is isothermal, thus approximations related to combustion and heat transfer are not needed.

The turbulent sub-grid scale stress terms in FDS are modeled with the standard Smagorinsky model with the SGS scale eddy viscosity calculated by:

$$\mu_{sgs} = \bar{\rho}(c_s\Delta)^2 |D| \quad (16)$$

where $\bar{\rho}$ is the filtered density, c_s the Smagorinsky constant, $|D|$ the filtered strain rate and Δ the filter width, defined the same as in FireFOAM. For the FDS simulations the standard Smagorinsky constant was set to $c_s = 0.1$.

The gradient diffusion hypothesis model is used for closing the un-resolved SGS species flux, assuming a constant turbulent Schmidt number of $Sc_t = 0.5$ [11].

In order to be consistent with the comparison of the two codes, the baroclinic torque due to the non-alignment of the density and pressure gradients that is incorporated in the momentum equation of FDS was not included. However, in simulations performed with the inclusion of the baroclinic torque (not shown here) the results did not differ much.

Experimental case

In this study comparisons are made with experiments performed in a large building designed for indoor fire experiments: the Fire Laboratory for Accreditation of Models and Experiments (FLAME) at Sandia National Laboratories in Albuquerque, New Mexico, and reported by O'Hern et al. [9].

The FLAME chamber is nominally a 6.1 m cubical enclosure with a 2.4 m in diameter chimney located on top of the chamber. The experiment was designed to be a canonical buoyant plume so that the results would be of use beyond the specific geometry that was used. Buoyant flows require a minimum scale to become fully turbulent that is typically much larger than for momentum-driven flow. Unlike momentum-driven flows, where vorticity is generated along the flow boundaries, turbulence in buoyant driven flows is primarily generated within the interior of the flow through a baroclinic mechanism. Also unlike momentum-driven flows, in which the distance to transition to turbulence can be shortened by increasing the inlet velocity at a fixed scale, in buoyant flows the baroclinic vorticity generation cannot be arbitrarily increased since it is determined by the pressure gradient and density gradient in the flow. The only way to reduce the distance to transition in a buoyant flow is to reduce its scale.

The plume source is 1 m in diameter and is surrounded by a 0.51 m wide floor, the "ground plane". The 1 m source diameter is chosen to ensure that the plume would be fully turbulent based on the pool fire fuel burn rate data of Blinov & Khudyakov et al. [15]. A detailed analysis of the spatial velocity distribution (average measurement spacing is 9 cm) of the plume inlet (using air instead of helium) shows that the inlet velocity profile is uniform to within $\pm 6\%$ [16]. The plume was developed using helium issuing form the diffuser at an average velocity of 0.325 m/s. For PLIF measurements, acetone was used as the fluorescent tracer gas, seeded into the helium flow at $1.7 \pm 0.1\%$ vol. In addition $1.9 \pm 0.2\%$ vol. oxygen was added to quench acetone phosphorescence. The molecular weight of the helium/acetone/oxygen mixture was $5.45 \pm 2.7\%$ g/mol. The average mixture Reynolds number was $\mathrm{Re} = DV_o / \nu = 3200 \pm 0.6\%$, where D is the diameter of the plume source (1 m), V_o is the inlet velocity and ν the kinematic viscosity of the helium/acetone/oxygen mixture. The average mixture Richardson number was $Ri = (\rho_\infty - \rho_p)gD / (\rho_\infty V_o^2) = 76 \pm 6.5\%$ with ρ_∞ the external (air) density, ρ_p the plume fluid density and g the acceleration due to gravity. The experiment was performed at a low ambient pressure of $P_\infty = 80900\,Pa$ due to the high altitude in which the facility is located and at a temperature of $T_\infty = 285\,K$.

The experimental uncertainty on the measured velocities and turbulent statistics are in the order of 20% and 30%, respectively. The values of concentration contain uncertainties in the

order of 18%, plus fixed uncertainties of 5%, while the concentration fluctuation in the order of 21%. The above uncertainties also include run-to-run variability [9].

Numerical setup

The simulations have been configured to replicate the experimental axisymmetric helium - air plume study of O'Hern et al. [9]. The experimental set-up for all the simulations is simplified into an $4\times4\times4m^3$ enclosure, shown schematically in Figure 2. A 1 m in diameter inflow of helium is used surrounded by a 0.5 m wide wall plate, which simulates a "ground plane" causing air being entrained by the accelerating plume to flow radially inward over the plate. The rest of the bottom plane injects a small co-flow of air. The plume inlet is located at the center of the bottom plane and is constructed by rectangular grid using a stair-step approximation of the circular geometry keeping the area as close as possible to the experimental dimensions. The grid resolution for all simulations is set to $160\times160\times160$ (≈ 4.1 million cells).

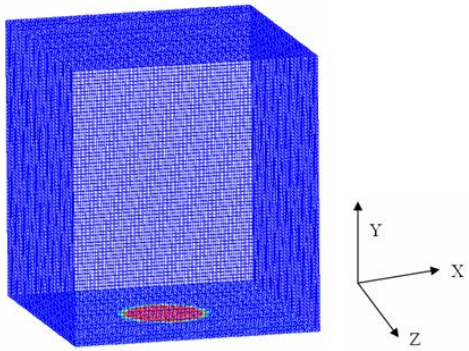

Figure 2. Schematic of computational domain showing the fuel inlet at $y=0\,m$

In FireFOAM the governing equations are advanced in time using a second order implicit "backward" scheme. Spatial derivatives are estimated on a rectangular grid with all quantities assigned to the cell center and velocities linearly interpolated to the cell faces. The convective terms are central differenced using a second order linear scheme. No purely upwind schemes were used since the use of unwinding in LES can introduce undesirable artificial numerical dissipation as has been noted by many studies [17]. This was also noted in the present study where different schemes were tested for discretizing the convective terms and it was evident in the simulations that any blending of the linear scheme with upwind resulted in high levels of numerical dissipation. For scalar transport the bounded second order TVD scheme, "limitedLinear01", is used and the diffusive terms are central differenced. A PISO algorithm is used for the pressure - velocity coupling and a Rhie-Chow correction to avoid odd-even decoupling errors appearing in regions of the flow where the Mach number approaches zero [18]. A linear GAMG solver solves the pressure equation.

The bottom plane of the domain at $y=0\ m$ employs a no-slip boundary for the cross-stream velocities and fixes the streamwise velocity of the inlet to $U^{f}_{inlet}=0.325\ m/s$ in the core of the plume and to a small co-flow velocity $U^{air}_{co-flow}=0.01\ m/s$ outside the plume. A "zeroGradient" BC is assigned for velocity at the sides of the domain and "totalPressure" BC for pressure. For the top outlet plane an "inletOutlet" BC is used for velocity and "zeroGradient" for pressure. The "inletOutlet" BC assigns a "zeroGradient" for outward velocity and fixes the inlet velocity to zero. The inlet BC for the mass fraction of 'fuel' is set to uniform "fixedValue 1.0". Inlet SGS kinetic energy is assigned the value

$k = 1.58 \cdot 10^{-7}\, m^2/s^2$ assuming a turbulent intensity of $I_u = 0.1\%$ [4] and $k = 1.0 \cdot 10^{-8}\, m^2/s^2$ for the ambient air. Details on the implementation of the BC's can be found in [10].

In FDS the governing equations are advanced in time by using a second order explicit "Runge-Kutta" scheme. Spatial derivatives are estimated with second order finite differences on a rectangular grid, with scalar quantities assigned to the cell center and velocities assigned to the cell faces. Convective terms are upwind biased, based on a Courant-Friedrichs-Lewy condition, in the predictor step and downwind biased in the corrector step. If the Courant number is near unity this corresponds to a nearly fully upwind scheme, while for Courant number much less than unity the scheme is more centralized. This second order finite differencing scheme of FDS cannot however fully resolve sharp gradients on a relatively coarse grid. Steep gradients can cause local over-shoots and under-shoots in quantities like density and species mass fraction. For this reason a flux correction scheme is performed in both the predictor and corrector steps to ensure that the quantities stay bounded. The second order TVD scheme, "SuperBee", is used for scalar transport and the diffusive terms are central differenced. A fast Fourier transform based solver solves the Poisson equation. All surfaces of the computational domain, co-flow area, sides and outlet are modelled as openings.

At every point in the domain, the composition of the gas phase corresponds to a mixture of fuel and air streams. The air stream has molecular weight $W_{air} = 28.9\ g/gmol$ while the experimental 'fuel' mixture of helium (He, 96.4% by vol.), acetone (CH_3COCH_3, 1.7% by vol.) and oxygen (O_2, 1.9% by vol.) is treated as a single gas with molecular weight $W_f = 5.45\ g/gmol$. Ambient (inlet) temperature and pressure are $T_\infty = 285\,K$ and $P_\infty = 80900\,Pa$, respectively, to match the experimental conditions. The Reynolds and Richardson numbers were $\mathrm{Re} = 3220$ and $Ri = 75.3$.

The LES calculations are set up to run for 20 seconds and collect data every 0.02 seconds in the simulation. The first 10 seconds allow for the initial computational flow transients to move downstream and to reach quasi-steady flow conditions. Results from the final 10 seconds of the simulation are compiled to produce density-weighted, time-averaged quantities. A constant time step is used in the simulations, corresponding to an average Courant number of $c_s \approx 0.2$.

Results and discussion

Figure 3 presents time traces of the centerline streamwise velocity at location $y = 0.5\,m$ above the inlet for a total of 4 sec in the simulation.

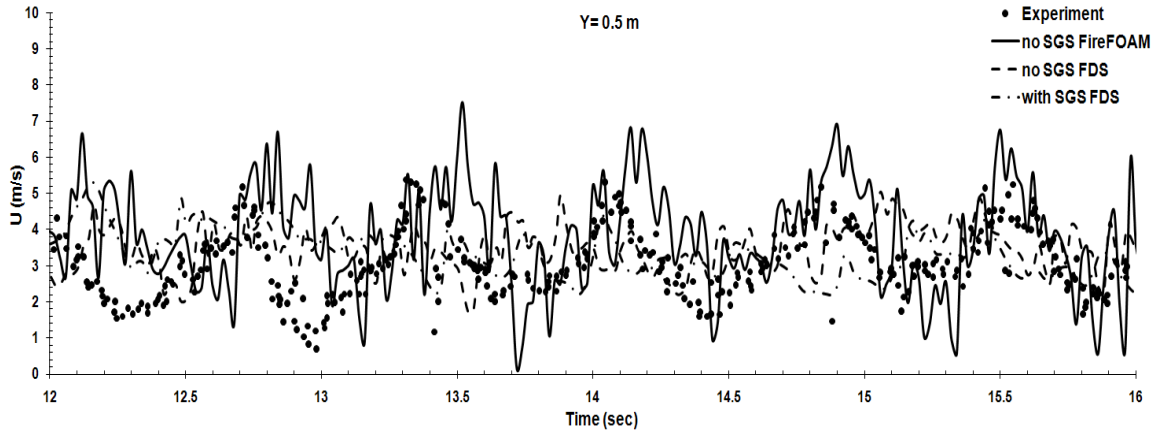

Figure 3. Time trace of centerline streamwise velocity at height $y = 0.5\,m$

The puffing frequency corresponds to the number of puffing cycles encountered, a maximum peak in the streamwise velocity followed by a minimum, in the given timeline examined. With FireFOAM a clear puffing frequency is observed. A total of 6 cycles, corresponding to the passage of large turbulent structures, are distinguished, and followed by an occasional smaller puff. With FDS no clear puffing frequency is evident, either with or without the use of SGS model. When the SGS is applied, a reduction in the dynamic range of the streamwise velocity occurs. Similar behaviour is also reported in [13].

A Fourier transformation on the time signal, taken for 10 puff cycles, of the streamwise velocity on the centerline at $y = 0.5m$ is presented in Figure 4. The software package Grace [19] was used for this purpose. FireFOAM predicts a puffing frequency of 1.38 Hz without SGS model. The observed puffing frequencies are in good agreement with the experimental correlation, $f = 0.8Ri^{0.38}U_p / D_p$, suggested by Cetegen et al. [5] for $Ri < 100$, which leads to a puffing frequency of 1.34 Hz for the set-up at hand and the frequency of 1.37 ± 0.1 Hz obtained by O'Hern et al. [9]. The frequencies are also in good agreement with the established puffing frequency correlations for buoyant diffusion flames of various fuels by Cetegen et al. [4], $f = 1.5/\sqrt{D_p}$, which yields a frequency of 1.5 Hz, independent of flow conditions. FDS doesn't predict a clear puffing frequency, either with or without the use of SGS model.

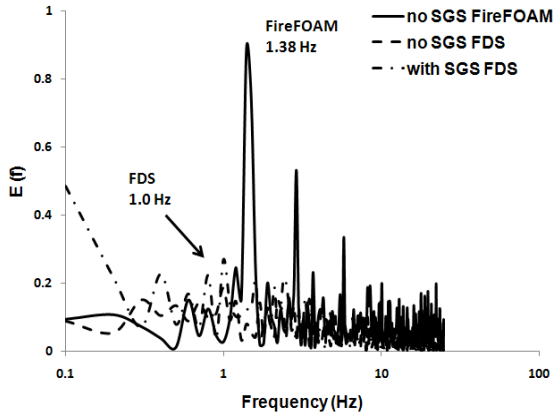

Figure 4. Power spectrum of streamwise velocity on the centerline at height $y = 0.5m$

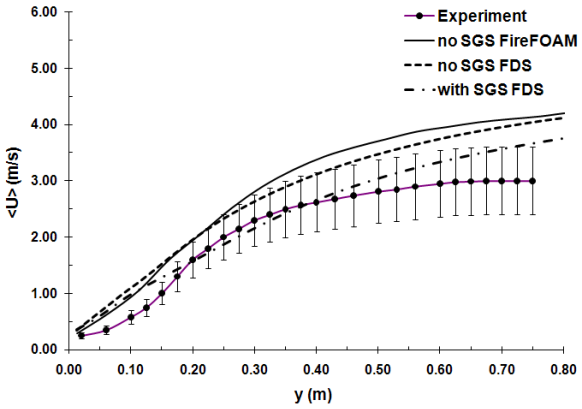

Figure 5. Comparison of mean centerline streamwise velocity

Figure 5 presents the centerline profiles of mean streamwise velocity up to $y = 0.8\ m$ above the base of the plume. Best agreement is observed for FDS with the use of SGS model. For this case, the laminar to turbulence transition is quite well captured and the simulation results remain with experimental uncertainty. The other cases predict a faster transition to turbulence and over-predict the mean streamwise velocity at locations higher than y=0.4 m.

Results for the density-weighted, time-averaged streamwise velocities at several heights (0.2 m, 0.4 m and 0.6 m above the inlet) are presented in Figure 6. For the cases without SGS model, the results are similar. The mean streamwise velocities predicted, are close to the experimental uncertainty for both FireFOAM and FDS. The use of SGS model in FDS damps the flow, leading to a decrease in the mean velocity, as reported also in DesJardin et al. [13].

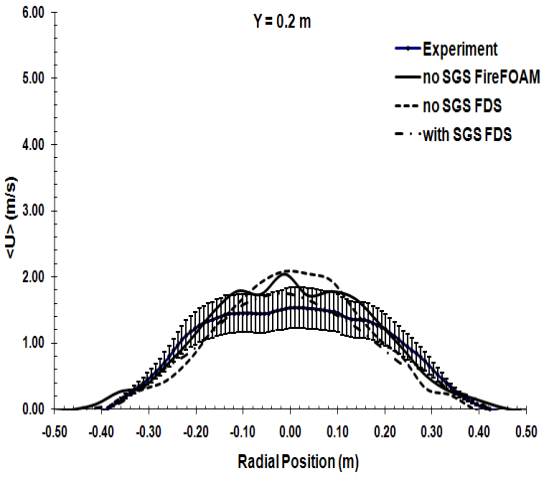

(a)

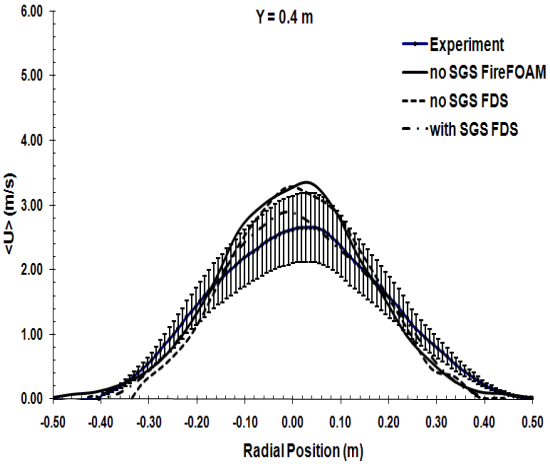

(b)

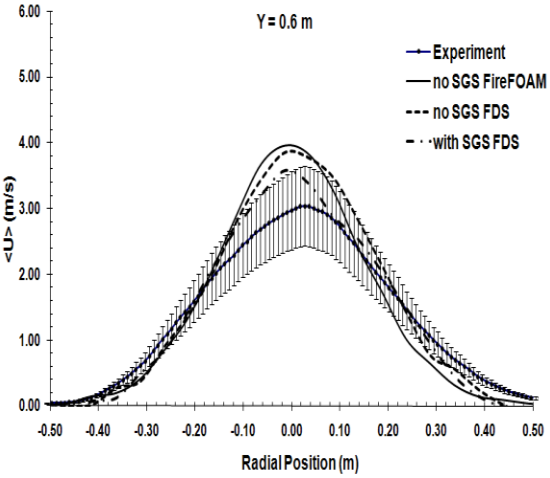

(c)

Figure 6. Comparison of time-averaged, density-weighted streamwise velocities at heights $y =$ (a) 0.2 m, (b) 0.4 m and (c) 0.6 m

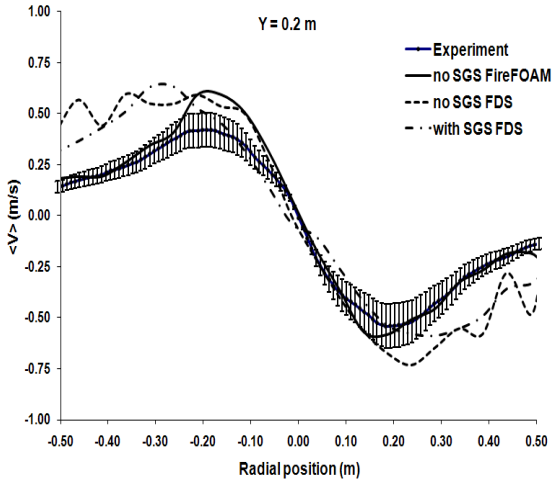

(a)

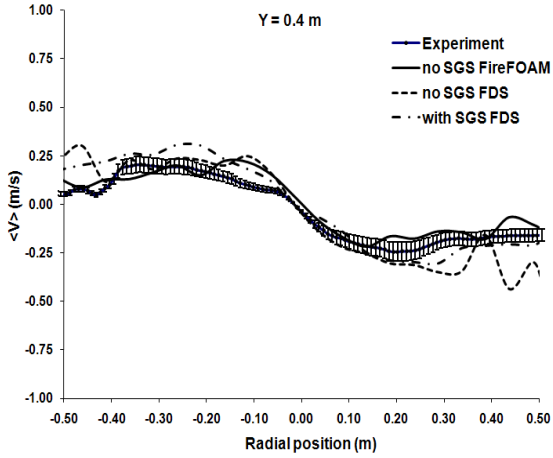

(b)

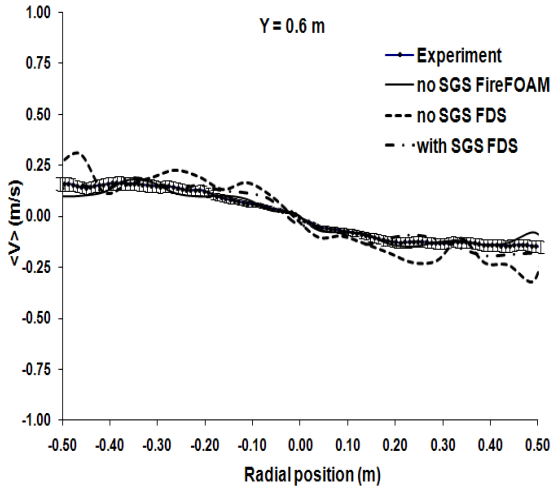

(c)

Figure 7. Comparison of time-averaged, density-weighted cross-stream velocities at heights $y =$ (a) 0.2 m, (b) 0.4 m and (c) 0.6 m

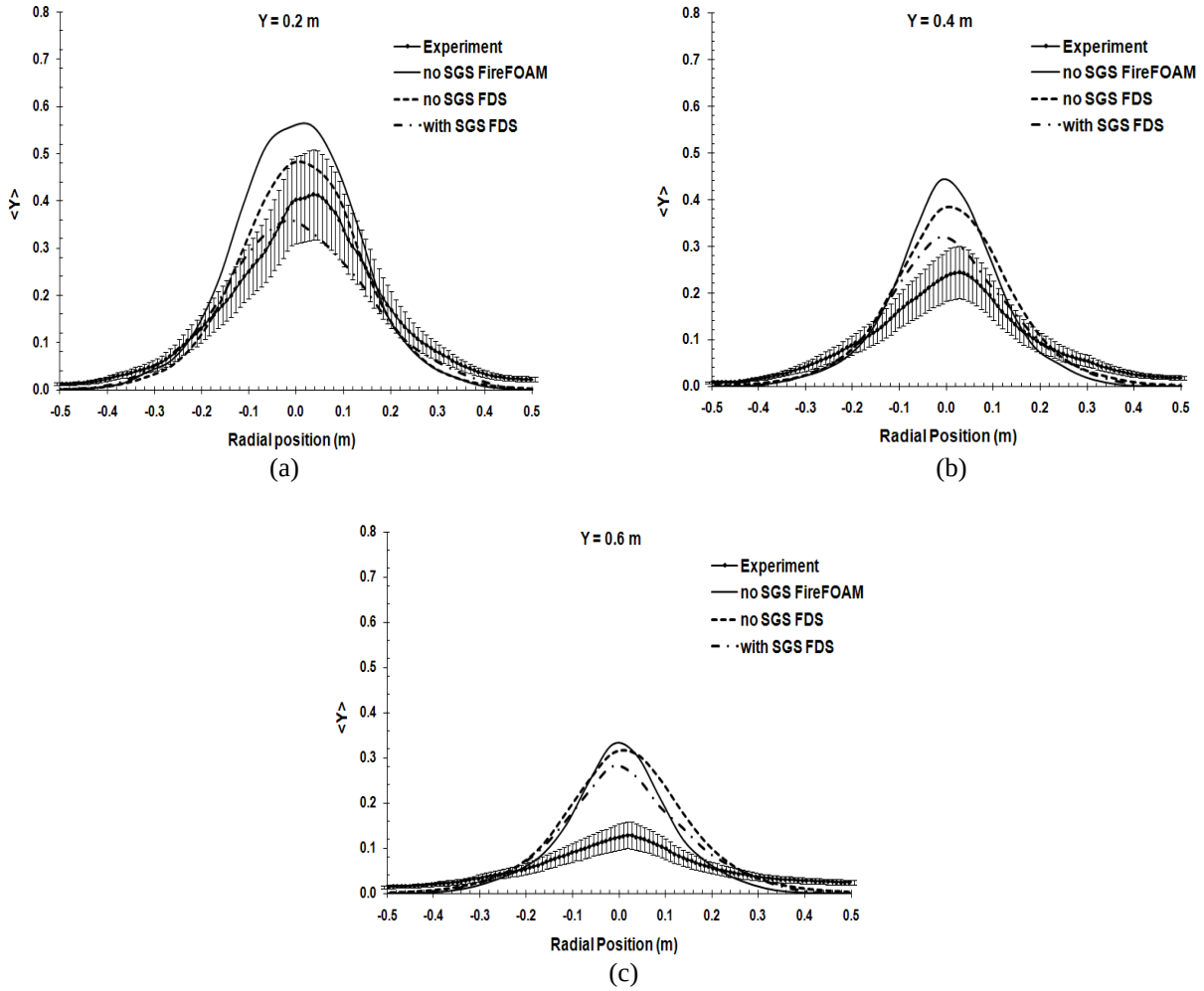

Figure 8. Comparison of time-averaged, density-weighted helium mass fractions at heights $y =$ (a) 0.2 m, (b) 0.4 m and (c) 0.6 m

Best agreement is observed by FDS with the use of SGS model. With this configuration, the predicted streamwise velocity matches well the experimental data at all heights. Also noticeable is that downstream, away from the plume inlet, there is an increase in the streamwise velocity and a decrease in the width of the velocity profiles, due to acceleration caused by buoyancy forces.

For the cross-stream velocities, presented in Figure 7, best agreement with the experiment is observed with FireFOAM without the use of SGS model. The simulation results match well the experiment data at all heights and the entrainment rates are well predicted. On the left hand side of the source, at location $x = -0.2\,m$, an over-prediction of the simulation results is observed. However, the experimental data at this location are not symmetric. For obvious reasons, the simulations cannot obtain this asymmetry. On the other hand, FDS simulations are not able to predict the correct entrainment rates. A great over-prediction of the cross-stream velocities is observed at all heights, at the source edge. This over-prediction is also present as we move towards the centreline. The application of a SGS model causes a decrease in the cross-stream velocity at all three heights. This is in line with streamwise velocity results presented in Figure 6. As a consequence of mass conservation, an increase in the cross-stream velocities will result in an increase in the streamwise velocities. Similarly, a decrease will result in decreased streamwise velocities. Accurate results for the cross-stream velocities are

important because in this kind of flows entrainment controls mixing, a very important parameter in pool fires where combustion processes are mixing-controlled.

Figure 8 presents results of the density-weighted, time-averaged helium mass fractions. The mean mass fraction of helium is over-predicted on the centerline, with larger discrepancies higher in the domain for all cases. This is due to lack of diffusion. Without SGS model, diffusion is under-estimated. This is seen when Figure 6 is also considered: the large differences in Figure 8 cannot simply explained by differences in (mean) convection. Figure 7 reveals the effect of the large cross-stream velocities in FDS, they lead to much more entrainment of air in FDS and thus lower mass fraction values of helium. Higher in the flow, differences remain small. Increasing the diffusion in the scalar transport equation and/or including effects of differential diffusion would improve the results. This would then imply the treatment of fuel as 3 components (helium, air and acetone), not as a mixture with a single diffusion coefficient, as was done here. Helium diffuses more easily than the other components, so a lower peak value on the centerline is expected. This is, however, beyond the scope of the present study. Best results are obtained, at all three locations, with FDS with the use of a SGS model.

Conclusions

In this study LES results obtained with FireFOAM and FDS for a buoyant large helium plume were presented.

For the mean streamwise velocities better agreement was obtained with FDS when the SGS model was applied. This configuration also presented the best laminar to turbulence transition. FireFOAM obtained best agreement for the mean cross-stream velocities. FDS was not able to capture correctly the entrainment rates close to the inlet, near the edge of the plume. Equally important, the resulting frequency for FireFOAM is in good agreement with the experiments and well-known correlations, which FDS was not able to capture the correct puffing frequency. For the helium mass fraction, at all locations, an over-prediction on the centerline is observed. This is due to lack of (differential) diffusion. Best agreement is observed with FDS and SGS model, but this could be for the wrong reasons (over-prediction of cross-stream velocities).

Overall, the quality of the results is comparable to results previously published in the literature [11, 13] with other CFD packages, which is encouraging for the use of FireFOAM in future work for simulations of fire-induced flows. A recent, more extensive, numerical study with FireFOAM, [20], supports this claim.

Acknowledgements

This research has been funded by Ghent University (Belgium) through BOF project 01J01909. The help of Yi Wang from FM Global concerning FireFOAM is greatly acknowledged. Also valuable, were the discussions taken in the annual FM Global Open Source CFD Fire Modeling Workshop concerning FireFOAM and fire-related research topics.

References

[1] http://code.google.com/p/firefoam-dev
[2] http://fire.nist.gov/fds/
[3] Burton, G. C., “Large eddy simulation of a turbulent helium-air plume using the nLES method”, *Center for Turbulence Research, Stanford University and NASA-Ames Research Center, Stanford, CA*, (2009)
[4] Cetegen, B. M., Ahmed, T. A., “Experiments on the periodic behavior of buoyant plumes and pool fires”, *Combustion and Flame*, 93:157–184 (1993)

[5] Cetegen, B. M., Kasper, "Experiments on the oscillatory behavior of buoyant plumes of helium and helium-air mixtures", *Physics of Fluids*, 8:2974–2984 (1996)
[6] Nicolette, V. F., Tieszen, S. R., Domino, S. P., Black, A. R., O'Hern, T. J., "A Turbulence model for buoyant flows based on vorticity generation", *Technical Report SAND2005-6273, Sandia National Laboratory, Albuquerque, NM* (2005)
[7] Tieszen, S. R., Domino, S. P., Black, A. R., "Validation of a simple turbulence model suitable for closure of temporally-filtered Navier-Stokes equations using a helium plume", *Technical Report SAND2005-3210, Sandia National Laboratory, NM* (2005)
[8] Van Maele, K., Merci, B., "Application of two buoyancy-modified k-e turbulence models to different types of buoyant plumes", Fire Safety Journal, 41: 122-138 (2006)
[9] O'Hern, T. J., Weckman, E. J., Gerhart, A. L., Tieszen, S. R., Schefer, R. W., "Experimental study of a turbulent buoyant helium plume", *J. Fluid Mech*. 544: 143-171 (2005)
[10] http://www.openfoam.com
[11] Chung, W., Devaud, C. B., "Buoyancy corrected k-ε models and large eddy simulation applied to a large axisymmetric helium plume", *Intl. J. Num. Meth. Fluids* 10.0012/fld.1720 (2008)
[12] Poinsot, T., Veynante, D., *Theoretical and Numerical combustion*, Edwards, 2001
[13] DesJardin, P. E., O'Hern, T. J., Tieszen, S. R.," Large eddy simulation and experimental measurements of the near-field of a large turbulent helium plume", *Phys. Fluids* 16: 1866-1883 (2004)
[14] Anderson, D. A., Tannehill, J. C., Pletcher, R. H., "Computational Fluid Mechanics and Heat Transfer", *Hemisphere Publishing Corporation*, Philadelphia, Pennsylvania, (1984)
[15] Blinov, V., Khudiakov, G. N., "Diffusive burning of liquids", *Technical Report T-1490a-c, ASTIA, AD296762, U.S. Army Engineering Research and Development Laboratories* (1961)
[16] Blanchat, T. K., "Characterization of the air source and plume source at FLAME", *Technical Report SAND01-2227, Sandia National Laboratory, Albuquerque, NM* (2001)
[17] Moin, P., "Advances in large eddy simulation methodology for complex flows", *Int. J. Heat Fluid Flow* 23: 710 (2002)
[18] Hirsch, C., "Numerical and Computation of Internal and External Flows", *Wiley*, New York, (1984)
[19] http://plasma-gate.weizmann.ac.il/Grace/
[20] Maragkos, G., Rauwoens, P., Merci, B., "Large eddy simulations of the flow in the near-field region of a turbulent buoyant helium plume" (submitted for publication)